Optimization of reactive element additions to improve oxidation performance of alumina-forming alloys*

Bruce A. Pint
Metals and Ceramics Division
Oak Ridge National Laboratory
Oak Ridge, TN 37831-6156

Abstract

It is well known that the addition of reactive elements (Y, Zr, La, Ce, Hf...) improve the high temperature oxidation performance of alumina-forming alloys. Less studied are strategies for optimizing these additions for developing a high-performance, wrought FeCrAl alloy with maximum oxidation-limited component life. Results from the literature are summarized regarding potential improvements. One promising strategy is the addition of two reactive elements, such as Y and Hf, which has been effective in commercial and laboratory Ni-base alloys and appears to impart the expected benefits, such as reducing the scale growth rate, while minimizing detrimental effects such as the formation of reactive element-rich oxides in the scale and internal oxidation. While there are promising data, the long term studies are not yet complete and it is difficult to predict if "co-doped" FeCrAl alloys will produce superior oxidation-limited lifetimes in high temperature environments.

*This research was sponsored by the U.S. Department of Energy, Office of Fossil Energy, Advanced Research & Materials Program under contract DE-AC05-00OR22725 with UT-Battelle, LLC.

Keywords: FeCrAl, Reactive elements, Co-Doping, Alumina Scales, High-temperature oxidation

Introduction

Studies of the effects of reactive elements (RE) on the oxidation behavior of FeCrAl-type alloys have been on-going for 40 years.[1-57] This type of alloy is of interest not only for application as heating elements and as catalyst supports for both automotive catalytic converters[28,32,41,51,56,57] and catalytic

combustion, but also as a model alumina-former. Many of the early studies sought to explain the RE effect by comparing the performance of RE-doped alloys to undoped alloys. This type of work produced numerous hypotheses about the RE effect[58-62] and has greatly increased the level of understanding about critical factors important for the formation, growth and adhesion of alumina scales. More recent studies have used ^{18}O tracers,[29,34,63-65] photo-stimulated laser spectroscopy (PSLS)[47,48] and transmission electron microscopy (TEM)[19,20,34,35,38,40,42,45,49,51,53,54,56] to more carefully study the RE effect. However, these comparative or mechanistic studies rarely discussed the relative performance of RE additions or how to optimize the effects for alloy development.

In recent years, the desire for higher operating efficiencies of energy systems has increased temperatures to the point where alumina-forming alloys are needed to fill critical material roles. With this increased attention comes the need to apply the collective database of information about alumina scale formation for alloy development. This paper attempts to outline some of that data which show that the simple addition of 0.05-0.1at.%Y to FeCrAl results in an alloy with excellent oxidation performance. Yet based on commercial Ni- and Fe-base alloys, one promising strategy for further improving the performance of FeCrAl is the addition of two or more REs or "co-doping". Current results in this development plan are presented comparing the performance of a traditional FeCrAlY alloy to co-doped alloys. Results from Ni-base alloys also are outlined to illustrate some of the compositional guidelines that have been developed.

Experimental Procedure

All of the alloys studied were inductively melted and cast using a chilled copper mold and annealed for 4h at 1300°C in a sealed quartz ampule. As-cast alloy compositions are given in Table I and all compositions are given in atom percent. Coupons ≈15mm in diameter and 1.0-1.5mm thick were cut and polished to a 0.3μm finish. Reaction kinetics were measured using a Cahn model 1000 microbalance in dry flowing O_2. Average rates were obtained using three separate specimens exposed for 50, 100 and 200h at 1200°C. Mass changes were corrected for the evaporation of the Pt-Rh hangdown wire. Specimens masses were measured before and after oxidation using a Mettler-Toledo model AG245

balance.

Cyclic oxidation experiments were conducted either in an automated test rig where the specimens were hung from Pt-Rh wire in a flowing O_2 environment and cycled for 1h at temperature and 10min cooling or, for long-term cycles (100 or 500h), in laboratory air in a box furnace with specimens in individual alumina crucibles which capture any spalled oxide.[66] Specimen lifetimes were measured as the time to breakaway oxidation, i.e. the formation of iron oxide across the specimen thickness. The lifetimes were linearly normalized to a 1.5mm specimen thickness in order to standardize the comparison.[67] After oxidation, specimens were characterized by field emission gun, scanning electron microscopy (SEM) and electron probe microanalysis (EPMA) and were coated with Cu prior to sectioning for metallography.

Results

Analysis of Literature Data

A review of the literature looking for information about optimizing the RE effect revealed both a wealth of information and a dearth of relative comparisons. Many of the early studies simply compared some form of RE addition to an undoped alloy and concluded there was an improvement. Additions were made by alloying, oxide dispersions, ion implantation, various type of coatings, etc. Parabolic rate constants reported or calculated from the literature for MCrAl-type alloys are summarized in Figure 1. If multiple RE compositions were studied, the lowest rate was included in the graph. When oxidation performance as a function of alloy RE content was reported, there was a typical trend such as that shown in Figure 2. Specimen mass gain typically was minimized with relatively low RE additions, ≈300-500 ppma, while higher and lower additions produced higher mass gains. For the example given in Figure 2, the minimum mass gain after 100h at 1100°C indicated the lowest rate constant and this same pattern continued in testing to 2000h at 1100°C for Hf-doped NiAl, indicating that this was not a short-term effect.[69]

The most commonly used commercial RE additions, such as Y, Zr, Hf, Ce and La, have been studied the most extensively but there also have been screening tests for numerous elements, especially

the rare-earth elements, looking for exceptional dopants.[44,45,70] The results of one such screening[44,45] are shown in Figure 3. The normalized lifetimes at 1200°C in 1h cycles of FeCrAl alloys made using a powder metallurgy process and dispersed with various oxide dopants are shown as a function of the dopant cation size. There appeared to be some benefit with increasing dopant ion size but there was no strong correlation such as has been found with doped chromia-forming alloys.[62] A flaw with the oxide dispersion strengthened (ODS) FeCrAl results is that most additions were made at the level of 0.2cation% whereas, to truly compare the various dopants, each dopant content would need to be individually optimized. For example, Ce, Eu, Sc and Yb were obviously "overdoped" with 0.2% and produced poor results. The performance for alloys with 0.05%Hf and 0.02%La were observed to perform better than most of the other compositions. The general point is that many potential dopant elements have been considered and the commonly studied elements, like Hf and Y, continue to show the best potential for improving oxidation resistance.

Single-Doped Alloys

Based on the literature review, the set of alloys listed in Table I was made in order to establish baseline information for RE-doped FeCrAl performance. The baseline data to gauge performance included rate constants, normalized lifetimes and scale microstructural information. Performance was studied primarily at 1200°C but also characterized at 1000°, 1100° and 1300°C.[68] Additions included Y, Hf, Zr and mischmetal (a combination of Ce, La and Nd).

A comparison of the 1200°C parabolic rate constants, Figure 4, showed that most of the RE-doped FeCrAl alloys had a 2-3X lower rate than undoped FeCrAl ($1.4x10^{-11}g^2/cm^4s$). For comparison, several commercial FeCrAl alloys also are included in Figure 4. The laboratory alloy with a 0.05%Hf addition had the lowest rate constant ($2.9x10^{-12}g^2/cm^4s$) which was much less than the rates for Y alloy additions (e.g. $7.5x10^{-12}g^2/cm^4s$ for FeCrAl+0.08%Y). Figure 5 shows the difference in scale thickness for these two alloys after 200h at 1200°C. At the metal-scale interface and in the metal, there were protrusions or pegs which included RE-rich oxides and indicated internal oxidation. These internal oxides contribute to the mass gain and result in higher parabolic rate constants. As expected, the amount of internal oxidation decreases as the RE content is reduced and this results in lower rate constants. This was

observed for both Y and Hf additions, Figure 4. When Y was added as an oxide dispersion in the commercial ODS alloys, MA956HT and PM2000, there was a slightly lower rate constant than with a Y alloy addition, presumably since there would be no internal oxidation of Y in the ODS alloys to contribute to the mass gain. However, the Y_2O_3-containing ODS alloys still exhibited higher rate constants than FeCrAl+0.05%Hf. Thus, Hf-doping was most effective in reducing the scale growth rate in FeCrAl.

A slower scale growth rate is only one goal, since the scale also must be spallation resistant in order for a long service life to be achieved. After the scale spalls, reformation of the alumina scale consumes Al from the substrate which has a finite reservoir. For FeCrAl alloys and especially foils, the Al content can generally be depleted to near 0% before breakaway oxidation occurs.[52,71] Breakaway oxidation, or the formation of iron oxide due to Al depletion, signals the end of useful life as the alloy is quickly consumed. Figure 6 shows the normalized lifetime at 1200°C in 1h cycles for the same alloys shown in Figure 4. All of the alloys nominally contained the same Al content, ≈10at.%, and the lifetimes were normalized to a 1.5mm thickness, so that each of the alloys started with a similar reservoir of Al[72] allowing a reasonable comparison to be made. The baseline for undoped FeCrAl was 310 1h cycles and the increases in lifetime for the RE-doped alloys were a direct result of the effect of the RE dopant on the alumina scale growth rate and adhesion. For the first set of alloys, RE additions increased the lifetime by up to a factor of 30 for the alloy with 0.08%Y.

For determining alloy lifetime, the RE effect on scale adhesion appears to be much more important than the effect on scale growth rate. Even though the 0.05%Hf-doped alloy had the lowest oxidation rate constant, it had one of the shortest lifetimes of the doped alloys due to excessive scale spallation. In contrast, FeCrAl+0.08%Y exhibited a much faster growing scale but had an exceptional lifetime of over 9000h, Figure 6. There was no clear reason for the poor spallation performance of the Hf-doped FeCrAl. It had a higher S content than some of the other RE-doped FeCrAl alloys and indigenous S has been linked to alumina scale spallation[24-26,28,37,73-76] but it is difficult to draw a direct correlation for this material. The commercial ODS alloys, PM2000 and MA956HT, contained 34 and 80ppma S, respectively and exhibited longer lifetimes than the Hf-doped material. Also, the HfO_2-

dispersed FeCrAl that had a lifetime of 2970h had a S content of 40ppma,[45] Figure 3.

The results from the first set of alloys showed two trends. First, that the indication from the literature that Hf additions may be superior in performance to Y additions was not observed for FeCrAl. (However, Hf additions are superior to Y additions for NiAl[50] and Fe_3Al.[77]) Second, that the performance of Y-doped FeCrAl is exceptional and simply optimizing the Y content may be the best solution for developing a high-performance FeCrAl alloy. However, optimizing the Y content did not produce the best performance in NiCrAl alloys[78] and the experience from that work may apply to FeCrAl alloys as well.

Co-Doped Alloys

Commercial NiCrAl-type alloys such as Haynes alloy 214 and the General Electric single-crystal superalloy René N5 both contain multiple reactive elements. Both have small Y additions (<100ppm) in addition to 120ppm Zr in alloy 214 and 500ppm Hf and ≈50ppm Zr in N5. This co-doping strategy with Y and Hf also has been practiced in commercial NiCoCrAl coatings.[79] The low level of Y used in these alloys would normally not be effective in improving scale adhesion on NiCrAl alloys.[78] However, in conjunction with a second element, excellent oxidation performance was achieved. An example for Ni-20Cr-19Al alloys[80] is given in Figure 7. In that case, alloys with only Y or Hf showed mass losses (indicating significant scale spallation) at 1100°C after 150 and 20 1h cycles, respectively. In contrast, a co-doped alloy with 60ppma Y and 460ppma Hf did not show mass losses until after 800 cycles. This behavior was similar to that of René N5. Again this behavior is difficult to attribute to S contents as the Y- and Hf-doped alloys both contained 8ppma S, the co-doped alloy has 5ppma and the René N5 ingot had 7ppma S. The Y and Hf together produced better results in a laboratory-made alloy and in commercial alloys with widely different Cr and Al contents.

This co-doping concept was applied to FeCrAl in several alloys, Table II, with varying success. Initially, Y and Hf were added at the same levels as in the first set of FeCrAl alloys. The alloy with 0.14%Y,Hf (0.09%Y and 0.05%Hf) exhibited a very high oxidation rate with a higher average parabolic rate constant at 1200°C than undoped FeCrAl, Figure 4. The reason for the increase was the formation of a large amount of internal oxidation. Figure 8a shows the internal attack on FeCrAl+0.14%Y,Hf after

200h at 1200°C. Even more extensive internal attack occurred after 10, 100h cycles at 1200°C, Figure 9b, extending more than 600µm into the substrate. For comparison, the depth of internal attack was only 125µm for FeCrAl+0.08%Y, Figure 9a. While the surface scales were similar in thickness on these two alloys, the mass gain after 1000h at 1200°C for the co-doped alloy was 8.85mg/cm^2 and only 3.68mg/cm^2 for FeCrAlY indicating the extent of the internal attack. Despite this large amount of internal attack, the normalized lifetime of the alloy was almost 4000h, exceeding many of the first set of alloys examined, Figure 6. Its lifetime suggests that it was not subject to the accelerated attack suggested for internally oxidized NiCoCrAlY coatings[81] and despite obvious over-doping, the alloy still showed promise.

The commercial Ni-base alloys suggested that the path for further improvement was to reduce both the Y and Hf contents of the alloy, but primarily the Y content because of its low solubility in the alloy. An alloy with 0.038%Hf,Y was produced, Table II, which showed relatively low scale growth rates at 1200°C (5.6×10^{-12}g^2/cm^{4}s) and greatly reduced internal attack, Figures 8b and 9c. For this alloy, the internal oxidation extended only to ≈40µm after 1000h at 1200°C. However, this result suggested that a further reduction in RE content may be possible and beneficial. A third co-doped alloy was made that contained only 0.020%Hf,Y, Table II. This alloy was the best performing of the co-doped alloys with a low average scale growth rate at 1200°C (3.5×10^{-12}g^2/cm^{4}s) close to the Hf-doped FeCrAl, Figure 4. Figure 10 shows the isothermal mass gain data at 1200°C for the progression of alloys from undoped to co-doped and illustrates the drop in mass gain from the undoped alloy to the alloy with 0.020%Hf,Y. Comparison of the scale thicknesses of the co-doped alloys in Figures 8 and 9 shows the benefit of minimizing the RE addition in reducing the scale growth rate, particularly between the 0.038% addition and the 0.020% addition, Figures 9c and 9d. Also, the amount of internal attack was further reduced to ≈20µm for the alloy with 0.020%Hf,Y after 1000h at 1200°C. A reduction in the parabolic rate constant also was observed over the range 1000°-1300°C, Table III.

The co-doping strategy successfully reduced the scale growth rate of FeCrAl but an improvement in lifetime has yet to be determined, as testing is still underway (arrows in Figure 6). The Y-Hf co-doped alloys have exceeded the lifetime of many of the first set of alloys including several commercial alloys,

but have yet to exceed the lifetime of FeCrAl+0.08%Y. It is interesting to note at this point that the mass change behavior of the co-doped alloys is different than that for the conventional alloys, Figure 11. While FeCrAl+0.08%Y showed mass losses between 1000 and 5000 cycles, the co-doped alloys still being tested show continued mass gains. This may suggest less scale spallation and a longer lifetime. Unfortunately, oxidation lifetime models[67,72,82] in their current state of development are not able to estimate the performance of these alloys, particularly because the cyclic oxidation performance of RE-doped FeCrAl alloys does not match that of Ni-base alloys for which the models were developed.[66]

A different indication about the long-term performance of the co-doped alloys is given by results from 100h cycles at 1200°C, where one of the co-doped alloys showed a scale spallation problem, Figure 12. For RE-doped FeCrAl in this test, the longer cycle time at temperature (i.e. decreased cycle frequency) would be expected to result in less scale spallation than 1h cycles (Figure 11) so that longer lifetimes are anticipated.[66] This test was terminated after 5,000h instead of testing to failure, because lifetimes over 25,000h were anticipated. In this test, the co-doped alloys showed lower total mass gains (specimen mass + spalled oxide) because of their lower scale growth rate compared to FeCrAl+0.08%Y. However, after 3500h, the specimen of FeCrAl+0.038Hf/Y showed a large amount of scale spallation (drop in specimen mass) resulting in a large increase in total mass as new scale was regrown. The specimen with 0.020%Hf/Y showed some limited spallation at the specimen edges after 4500h.

A similar test was conducted at 1100°C with 100h cycles, Figure 13. Again, the co-doped alloys have shown lower mass gains than FeCrAl-0.08%Y because of the slower scale growth rates. However, in this case, no significant scale spallation has been observed for any of the alloys.

The current results tend to suggest that even lower RE contents would continue the improvement in oxidation performance. However composition control with minor alloy additions can be problematic even on a laboratory scale. Of particular concern is that the raw materials, especially Cr, can contain large amounts of S and O. A fourth Hf-Y alloy, which was an attempt to achieve a lower total RE level, resulted in a lower Hf content (0.018%) but an undetectable Y content, Table II. The behavior of this material showed how abrupt the shift in performance can be when the RE content is changed as suggested by the data in Figure 2. This alloy showed a low scale growth rate, Figure 4, but such severe scale

spallation that there was almost no improvement in lifetime compared to undoped FeCrAl, Figure 6. One alloy also was made with Y and Zr additions, Table II. However, the Y level was below detection limits and the performance of the alloy was disappointing. It had an unexpectedly high scale growth rate, Figure 4, and a normalized lifetime of only 2310h at 1200°C, Figure 6. A Y,Zr co-doped alloy might be effective with a lower Zr level and higher Y content.

The last two co-doped alloys contained little or no Y, and higher S levels, which empirically have been linked to poor cyclic oxidation performance. Several authors have considered the ratio of dopants to impurities to be an important factor,[28,73,75,76,80] particularly the Y/S and Hf/C ratios. As there is only limited information with co-doped FeCrAl alloys, again, it is worth considering evidence from Ni-base alloys. Figure 14 shows the performance of a group of alloys with a base Ni-7Cr-13Al composition.[80] In this case, when only Hf was added to the alloy, spallation was observed after less than 100 1h cycles at 1100°C. Two alloys with only Y additions showed minor scale spallation after a few hundred cycles. Three co-doped alloys with S contents in the 25-35ppma range had Y/S ratios less than 1 and all showed scale spallation at short times. Co-doped alloys made with higher purity Cr had lower S (5-7ppma) and higher Y contents resulting in Y/S ratios much greater than 1. These alloys showed little scale spallation after 1000 cycles at 1100°C, Figure 14. Unfortunately, controlling the C content (and thus the Hf/C ratio) of the alloys was difficult. However, the Hf/C ratio in these alloys did not appear to be as critical a factor as it was in Hf-doped NiAl.[80] If these same ratios are calculated for the co-doped FeCrAl alloys, the two alloys with undetectably low Y levels have Y/S ratios less than 1. For the FeCrAl alloys containing Hf, all of the alloys had Hf/C ratios greater than 1 except for the last co-doped alloy with 0.018%Hf, which had poor performance. Empirically, these ratios appear to give some indication of performance and have been used as composition guidelines. However, their physical or mechanistic significance has not been clearly determined.

Discussion

These results demonstrate that it is possible to reduce the scale growth rate of FeCrAl alloys by manipulating the type and amount of RE addition. A major unanswered question is if these efforts can

produce a superior alloy in terms of oxidation-limited lifetime compared to Y-alloyed FeCrAl. Improved lifetime is the more critical factor for most commercial applications of RE-doped FeCrAl. However, commercial alloys have already utilized the concept in Ni-base (alloy 214 and René N5) and Fe-base (Krupp-VDM's Aluchrom YHf)[57] all of which exhibit excellent high-temperature oxidation resistance.

The fundamental premise for co-doping is to minimize the amount of Y (which is relatively insoluble in FeCrAl) and to supplement the Y with a sufficient amount of a more soluble RE like Hf or Zr. Tien and Pettit[5] suggested that the solubility limit of Y in FeCrAl was near 60ppma (0.01wt.%). Based on observations in these cast FeCrAl alloy, the solubility limit of Hf appears to be 200-300ppma. Confirmation of this assessment is that the 0.020%Hf/Y alloy contained no visible second phase particles and, upon annealing at 1300°C, the 16mm diameter casting generally contained one or two grains in section as there were no second phase particles to inhibit the growth of the alloy grains. By reducing or eliminating the RE-rich particles in the alloy, it is possible to reduce the amount of internal oxidation, oxide pegs and RE-rich oxides in the scale.

Effect on the α-Al_2O_3 scale growth rate

The co-doping strategy is effective in reducing the scale growth rate because the amount of RE-rich oxide particles in the scale and beneath the oxide are minimized. Rather than oxide particles, the beneficial effect of RE dopants is attributed to the segregation of RE ions at scale grain boundaries and the metal-scale interface.[61] Studies of the RE-doped α-Al_2O_3 scale growth mechanism using ^{18}O tracer experiments have found that it grows primarily by the inward grain boundary diffusion of oxygen.[29,63-65] All of the RE-doped FeCrAl alloys have a similar activation energy for the parabolic rate constant, Table III. This activation energy is considerably different than that measured for undoped FeCrAl. This suggests a similar growth mechanism for Y-doped and co-doped alloys. Many authors[5,20,54-57,83-85] have studied RE-rich oxides within alumina scales and their presence likely provides a fast oxygen diffusion path, either through the particle itself, along the particle-alumina interface, or because the particles are often accompanied by adjacent voids.[34,54-57,84-86] The presence of RE-rich oxide particles also could result in a higher concentration of RE ions on the scale grain boundaries resulting in faster boundary transport in the scale.[87] This could explain why reducing the Y_2O_3 content in ODS FeCrAl,

where internal oxidation does not occur, reduced the scale growth rate.[34]

The conclusion about RE-rich particles increasing diffusion through the scale also is based on the increased thickness of the scale near RE-rich particles incorporated in the oxide and the high oxygen diffusivity of most rare-earth oxides.[83] Because all RE dopants are less noble than Al, if their oxides formed low oxygen diffusivity oxides, a RE-rich oxide layer would be expected to form at the metal-scale interface, such as occurs for silica beneath chromia scales. The fact that this does not occur, and that RE-rich internal oxides are observed to be encapsulated in a sheath of alumina[83] indicates that they are fast oxygen conductors. Examples of alumina encapsulation can be seen in Figures 5, 8 and 9, where the RE-rich oxides appear lighter than alumina, e.g.arrows in Figures 5a, 8b and 8c. Their minimization in the alumina scale can thus be considered beneficial to forming a slow-growing scale. Doping with Hf may result in a slower growing alumina scale (Figures 4 and 5) than Y-doping because Y incorporation in the scale will lead to the formation of $Y_3Al_5O_{12}$ while Hf does not form a compound oxide with Al. Thus, the same amount of Hf in the scale will result in a smaller volume of HfO_2.

Effect on the α-Al_2O_3 scale adhesion

A co-doping strategy may not be ultimately effective in improving scale adhesion or at least in achieving a greater improvement in alloy lifetime as FeCrAl-0.08%Y, because minimizing the number and length of oxide pegs may have an adverse effect on scale adhesion. Since the first published work on FeCrAlY,[1] oxide pegs have been proposed to improve scale adhesion.[58] However, because of the excellent scale adhesion on ODS alloys, which do not form oxide pegs because the Y is added as an oxide, the pegging mechanism is often not given much consideration. There is a strong intuitive sense that oxide pegs are important to spallation resistance because of their potential to arrest crack propagation at the metal-scale interface. Inevitably, fracture will occur at this “weakest-link” interface and oxide pegs may limit the spallation to small areas. This would minimize the amount of scale loss and thus limit the Al consumption needed to regrow the spalled scale. However, the presence of oxide pegs, and particularly large $Y_3Al_5O_{12}$ particles, has been linked to increased scale spallation because of stress concentration and/or thermal expansion mismatch with the alloy and scale.[78,88]

The observation of spallation on the FeCrAl+0.038%Hf,Y alloy (Figure 12) may be due to the

reduced number of oxide pegs. However, spallation was observed in 100h cycles at 1200°C (Figure 12) but not in 1h cycles at 1200°C (Figure 11) or 100h cycles at 1100°C (Figure 13) which may indicate that the spalling is related to the longer cycle time and higher temperature. Short cycles could result in a large number of small defects while a longer cycle could impose a larger strain on cooling and also allow more time at temperature for defects to grow to a critical size between cooling cycles.[66] A few oxide pegs, as observed for FeCrAl+0.08%Y, e.g. Figure 9a, could result in a more spallation resistant alloy, especially in long cycles.

In general, FeCrAlY had a greater oxidation lifetime than the commercial ODS alloys at 1200°C by 2-3X, Figure 6. However, this difference has been linked to the benefit of stress relaxation in the weaker wrought material,[89,90] not just an effect of oxide pegs. Deformation of a weak substrate is thought to relieve stress in the scale, thereby reducing spallation. The low strength of FeCrAlY may give it exceptional spallation resistance but its lack of high temperature strength limits its application whereas ODS alloys offer both creep and oxidation resistance.

One issue that has not been explored is the possibility that with only a low level of RE addition that the alloy could effectively become depleted in RE dopant. Especially in cases where spallation occurs, if the RE tends to enrich itself in the scale, then the alloy may become depleted in RE. The current results on FeCrAl at 1200°C do not necessarily reflect this possibility but in 100h cycles at 1300°C, it has been observed that FeCrAl+0.08%Y has a 50% longer time to breakaway than FeCrAl+0.038%Hf/Y. Also, for Hf-doped Fe_3Al, in 100h cycles at 1300°C, an alloy with a 0.1%Hf addition had a 20% longer life than an alloy with 0.05%Hf while in 1h cycles at 1200°C, the same material had a 15% shorter life. This effect also may be related to the higher test temperature (1300°C) where there was less difference in scale growth rates with the different RE additions, e.g. Table III.

Effect of alloy impurities

A factor that may limit the commercial potential of co-doped FeCrAl alloys is the apparent need for good impurity control. The best alloys in this study were made using high-purity Cr and had relatively low S and C contents. In commercial alloys, it may be impractical or economically unfeasible to maintain such low levels of impurities. The need to control the C and N contents has been emphasized

in a number of studies[54-57,91] and the commercial co-doped FeCrAl (Aluchrom YHf) has only 2-3ppma S but also contains Hf, Zr and Ti which were selected to react with C in the alloy.[57]

The current results with low Y and Hf additions suggest that if the Y/S and/or Hf/C ratios are below 1, the alloy may have less than optimal performance. The same critical Y/S ratio was observed for René N5.[76] While there is empirical evidence suggesting that these ratios are important to cyclic oxidation performance, there is no strong mechanistic explanation. Smeggil and co-workers[24,26] suggested that Y gettered S, thus the apparent need for an excess (i.e. Y/S>1) addition. Sigler[28] suggested that RE additions react with not only S but also C, N and O and thus low additions of Hf and Y were less effective because they were tied up with impurities. However, both Y and S were detected by Auger electron spectroscopy at the metal interface when MCrAlY alloys were heated to 900°C.[25] It also has been shown that Y from oxide particles in ODS alloys ends up enriched at the gas interface of the scale after prolonged high temperature exposure.[35,38,45,49,50,61,84,85,92] Therefore, if oxide particles dissolve and diffuse in the alloy, then sulfides and carbides also should dissolve in a similar fashion. The gettering hypothesis needs to be more carefully studied.

A different interpretation of the importance of these ratios is that excess impurities may affect the RE activity in the alloy and thereby affect the rate at which RE dopants diffuse in the alloy and become enriched in the scale. In addition to RE-rich oxide forming within the scale, smaller RE-rich oxide particles nucleate at the scale-gas interface and grow during exposure.[38,45,49,50,61,92] It is one of the hallmarks of RE doping that those dopants that are effective in improving scale adhesion also diffuse outward during oxidation.[45] A study of the growth of these particles[92] found that the volume of HfO_2 or ZrO_2 particles at the scale-gas interface did not increase with Hf or Zr content in the NiAl substrate. This suggested that these particles were an inevitable consequence of the outward diffusion of RE ions from the alloy into the scale. However, a comparison of Hf and HfO_2 additions to NiAl found a noticeable decrease in HfO_2 particle volume at the scale-gas interface when Hf was added as an oxide[92] and a decrease in the beneficial effects.[50] Thus, in co-doped FeCrAl if Hf is tied up as a carbide or Y as a sulfide due to excessive alloy impurities, they may not be permanently gettered but rather limited in their ability to diffuse in the alloy and thus diffuse into the scale. This may be a particularly important point

when their concentration has been minimized.

Summary

The purpose of this work is to illustrate a strategy for optimizing the reactive element effect in wrought FeCrAl alloys based on the large literature database and current mechanistic understanding of RE effects in both Fe- and Ni-base alumina-forming alloys. Using single additions of Y, Zr, Hf and mischmetal as a baseline, it has been shown that co-doping FeCrAl with low levels of Y and Hf can produce an α-Al_2O_3 scale with a slower growth rate at 1000°-1300°C. It is believed that this reduction in the growth rate is not due to a change in the growth mechanism but due to a reduction in the volume of RE-rich oxides in the scale which accelerate scale growth. It also was shown that scale growth rate and the alloy lifetime, defined as the time to breakaway oxidation, are not strongly correlated. For determining lifetime, the RE effect on scale adhesion appears to be much more important than the effect on scale growth rate. Thus, reducing the scale growth rate will not necessarily result in an improvement in alloy lifetime. It has yet to be determined if these co-doped FeCrAl alloys will exceed the exceptional lifetime of FeCrAlY at 1200°C.

Acknowledgments

The authors would like to thank G. Garner, L. D. Chitwood, H. Longmire, T. Geer, J. W. Jones, L. Walker and K. S. Trent for assistance with the experimental work. P. F. Tortorelli and I. G. Wright provided helpful comments on the manuscript. This research was sponsored by the U.S. Department of Energy, Office of Fossil Energy, Advanced Research Materials Program under contract DE-AC05-00OR22725 with UT-Battelle, LLC.

References

1. C. S. Wukusick and J. F. Collins, "An Iron-Chromium-Aluminum Alloy Containing Yttrium," Mater. Res. Stand., 4 637-46 (1964).
2. J. M. Francis and W. H. Whitlow, "The Effect of Yttrium on the High Temperature Oxidation Resistance of Some Fe-Cr Base Alloys in Carbon Dioxide," Corr. Sci., 5 701-10 (1965).

3. J. E. Antill and K. A. Peakall, "Influence of an Alloy Addition of Y on the Oxidation Behaviour of an Austenitic and a Ferritic Stainless Steel in Carbon Dioxide," J. Iron .Steel Inst., 205 1136-4 (1967).
4. J. M. Francis and J. A. Jutson, “High Temperature Oxidation of an Fe-Cr-Al-Y Alloy in CO_2,” Corr. Sci., 8 445-9 (1968).
5. J. K. Tien and F. S. Pettit, “Mechanism of Oxide Adherence on Fe-25Cr-4Al (Y or Sc) Alloys,” Met. Trans., 3A 1587-99 (1972).
6. A. Kumar, M. Nasrallah and D. L. Douglass, "The Effect of Yttrium and Thorium on the Oxidation Behavior of Ni-Cr-Al Alloys," Oxid. Met., 8 227-63 (1974).
7. F. A. Golightly, F. H. Stott and G. C. Wood, "The Influence of Yttrium Additions on the Oxide-Scale Adhesion to an Iron-Chromium-Aluminum Alloy,” Oxid. Met., 10 163-87 (1976).
8. I. M. Allam, D. P. Whittle and J. Stringer, "The Oxidation Behavior of CoCrAl Systems Containing Active Element Additions," Oxid. Met., 12 35-66 (1978).
9. F. H. Stott, G. C. Wood and F. A. Golightly, “The Isothermal Oxidation Behavior of Fe-Cr-Al and Fe-Cr-Al-YAlloys at 1200°C,” Corr. Sci., 19 869-87 (1979).
10. F. H. Stott, F. A. Golightly and G. C. Wood, “The Influence of Thermal Cycling on the Oxidation Behaviour of Fe-Cr-Al and Fe-Cr-Al-Y Alloys at 1200°C,” Corr. Sci., 19 889-906 (1979).
11. I. M. Allam, D P Whittle and J Stringer, "Improvements in Oxidation Resistance by Dispersed Oxide Addition: Al_2O_3-Forming Alloys," Oxid. Met., 13 381-401 (1979).
12. M. J. Bennett, M. R. Houlton and G. Dearnaley, "The Influence of the Surface Ion Implantation of Al & Y upon the Oxidation Behavior of a Fe-15%Cr-4%Al FeCrAlloy Stainless Steel, in Air, at 1100°C," Corr. Sci., 20 69-72 (1980).
13. A. S. Khan, C. E. Lowell and C. A. Barrett, "The Effect of Zirconium on the Isothermal Oxidation of Nominal Ni-14Cr-24Al Alloys,” J. Electrochem. Soc., 127 670-9 (1980).
14. J. Nowok, “Formation Mechanisms of Keying or Pegging Yttrium Oxide and Increased Plasticity of Alumina Scale on FeCrAlY,” Oxid. Met., 18 1-17 (1982).
15. D. Delaunay and A. M. Huntz, "Mechanisms of Adherence of Alumina Scale Developed During High-Temperature Oxidation of Fe-Ni-Cr-Al-Y Alloys," J. Mater. Sci., 17 2027-36 (1982).
16. L. Zhang L, Y Yin, L Li, Q Zhao, B Zhang, “An Investigation of Residual Stress of Oxide Scale Affected by the Addition of Rare Earth Elements in Fe-Cr-Al Alloys at 1200°C and 1350°C,”; pp.267-73 in *High Temperature Corrosion*. Edited by R. A. Rapp. National Association of Corrosion Engineers, Houston, TX, 1983.
17. T. Amano, S. Yajima and Y. Saito, “High Temperature Oxidation of Fe-20Cr-4Al Alloys with Small Additions of Sc, Y, or Er,”; pp.247-54 in High Temperature Corrosion Transactions Supplement, v. 24, Proceedings of JIMIS-3, Japan Inst. Met., Tokyo, Japan, 1983.
18. M. H. Lagrange, A. M. Huntz and J. H. Davidson, "The Influence of Y, Zr, or Ti Additions on the

High Temperature Oxidation Resistance of Fe-Ni-Cr-Al Alloys of Variable Purity," Corr. Sci., 24 613-27 (1984).

19. T. A. Ramanarayanan, M. Raghavan and R. Petkovic-Luton, “The Characteristics of Alumina Scales Formed on Fe-Based Yttria-Dispersed Alloys,” J. Electrochem. Soc., 131 923-31 (1984).
20. T. A. Ramanarayanan, M. Raghavan and R. Petkovic-Luton, "Metallic Yttrium Additions to High Temperature Alloys: Influence on Al_2O_3 Scale Properties," Oxid. Met., 22 83-100 (1984).
21. P. T. Moseley, K. R. Hyde, B. A. Bellamy and G. Tappin, “The Microstructure of the Scale Formed During the High Temperature Oxidation of a FeCr Alloy Steel” Corr. Sci., 24 547-65 (1984).
22. T. T. Huang, Lin, D. A. Shores and E. Pfender, “Corrosion of FeCrAl, FeCrAlY, and FeCrAlHf Alloys in High Temperature H_2-H_2O-H_2S Environments,” J. Electrochem. Soc., 131 2191-6 (1984).
23. N. Pandey, S. Prakash and M. L. Mehta, “Effect of Zirconium on High Temperature Oxidation of Fe-15Cr-4Al Alloy,”; pp.389-93 in Proceedings of the 9th International Congress on Metallic Corrosion, Vol. 3. National Research Council of Canada, Ottawa, Canada, 1984.
24. J. G. Smeggil and A. J. Shuskus, “The Oxidation Behavior of some FeCrAlY, FeCrAl, and Yttrium Ion-Implanted FeCrAl Alloys Compared and Contrasted,” J. Vac. Sci. Tech. A, 4, 2577-82 (1986).
25. K. L. Luthra and C. L. Briant, “Mechanism of Adhesion of Alumina on MCrAlY Alloys,” Oxid. Met., 26 397-416 (1986).
26. J. G. Smeggil, “Some Comments on the Role of Yttrium in Protective Oxide Scale Adherence,” Mat. Sci. and Eng., 87 261-65 (1987).
27. G. B. Abderrazik, G. Moulin, A. M. Huntz, E. W. A. Young and J. H. W. de Wit, “Growth Mechanism of Al_2O_3 Scales Developed on FeCrAl Alloys,” Solid State Ionics, 22, 285-94 (1987).
28. D. R. Sigler, “Aluminum Oxide Adherence on Fe-Cr-Al Alloys Modified with Group IIIB, IVB, VB, and VIB Elements,” Oxid. Met., 32 337-55 (1989).
29. W. J. Quadakkers, H. Holzbrecher, K. G. Briefs and H. Beske, "Differences in Growth Mechanisms of Oxide Scales Formed on ODS and Conventional Wrought Alloys," Oxid.Met., 32 67-88 (1989).
30. M. J. Bennett and M. R. Houlton, “Comparison Between the Oxidation Behavior of FeCrAlloy Stainless Steel and the MA956 Oxide Dispersion Strengthened Alloy,”; pp.227-38 in *High Temperature Materials for Power Engineering*. Vol. B. Edited by E. Bachelet, R. Brunetaud, D. Coutsouradis, P. Esslinger, J. Ewald, I. Kvernes, Y. Lindblom, D. B. Meadowcroft, V. Regis, R. B. Scarlin, K. Schneider and R. Singer Kluwer Academic Publishers, Dordrecht, Netherlands, 1990.
31. J. Jedlinski, G. Borchardt, S. Mrowec, “The Influence of Reactive Elements on the degradation

of commercial Fe-23Cr-5Al alloys at High Temperatures," Werkst. Korros. 41 701-9 (1990).

32. T. Kawasaki and K. Ishii, "Development of Oxidation Resistant Fe-20Cr-5Al Foil for Automotive Catalytic Converter Use,"; pp.1205-11 in *Proceedings of the International Conference on Stainless Steels*. Iron and Steel Institute of Japan, Taokyo, Japan, 1991.
33. P. Y. Hou, Z. R. Shui, G. Y. Chuang and J. Stringer, "Effect of Reactive Element Oxide Coatings on the High Temperature Oxidation Behavior of a FeCrAl Alloy," J. Electrochem. Soc., 139 1119-26 (1992).
34. D. Clemens, K. Bongartz, W. Speier, R. J. Hussey and W. J. Quadakkers, "Analysis and Modeling of Transport Processes in Alumina Scales on High Temperature Alloys," Fresenius' J. Anal. Chem., 346 318-22 (1993).
35. B. A. Pint, A. J. Garratt-Reed and L. W. Hobbs, "The Effect of Y and Ti on FeCrAl Oxidation at 1400°C," J. Phys. IV, 3 C9-247-55 (1993).
36. V. K. Tolpygo and H. J. Grabke, "Microstructural Characterization and Adherence of α-Al_2O_3 Oxide Scales on Fe-Cr-Al and Fe-Cr-Al-Y Alloys," Oxid. Met., 41 343-64 (1994).
37. M. C. Stasik, F. S. Pettit, G. H. Meier, A. Ashary and J. L Smialek., "Effects of Reactive Element Additions and Sulfur Removal on the Oxidation Behavior of FeCrAl Alloys," Scripta Met. et Mater., 31 1645-50 (1994).
38. B. A. Pint, A. J. Garratt-Reed and L. W. Hobbs, "The Reactive Element Effect in Commercial ODS FeCrAl Alloys," Mater. High Temp., 13 3-16 (1995).
39. C. Forest and J. H. Davidson, "Some Observations on the Effects of Sulfur and Active Elements on the Oxidation of Fe-Cr-Al Alloys," Oxid. Met., 43 479-90 (1995).
40. G. Du, Z. Yann, J. Cai and Z. Xiao, "TEM Studies of Cross-Sections of Oxidized Fe-25Cr-6Al-La Alloy," Oxid. Met., 44 417-28 (1995).
41. A. Andoh, S. Taniguchi and T. Shibata, "High-Temperature Oxidation of Al-Deposited Stainless Steel Foils," Oxid. Met., 46 481-502 (1996).
42. C. Mennicke, E. Schumann, C. Ulrich and M. Rühle, "The Effect of Yttrium and Sulfur on the Oxidation of FeCrAl," Mat. Sci. Forum, 251-254 389-96 (1997).
43. B. Jönsson and C. Svedberg, "Limiting Factors for Fe-Cr-Al and NiCr in Controlled Industrial Atmospheres," Mat. Sci. Forum, 251-254 551-8 (1997).
44. B. A. Pint, "Study of the Reactive Element Effect in ODS Iron-Base Alumina-Formers," Mater. Sci. Forum, 251-254 397-404 (1997).
45. B. A. Pint and K. B. Alexander, "Grain Boundary Segregation of Cation Dopants in α-Al_2O_3 Scales," J. Electrochem. Soc., 145 1819-29 (1998).
46. V. K. Tolpygo and H. J. Grabke, "The Effect of Impurities on the Alumina Scale Growth: An Alternative View," Scripta Mater., 38 123-9 (1998).
47. V. K. Tolpygo, J R Dryden and D R Clarke, "Determination of the Growth Stress and Strain in α-

Al_2O_3 Scales During the Oxidation of Fe-22Cr-4.8Al-0.3Y Alloy," Acta Mater., 46 927-37 (1998).

48. V. K. Tolpygo and D R Clarke, "Competition Between Stress Generation and Relaxation During Oxidation of an Fe-Cr-Al-YAlloy," Oxid. Met., 49 (1998) p.187-212.
49. B. A. Pint, A. J. Garratt-Reed and L. W. Hobbs, "Possible Role of the Oxygen Potential Gradient in Enhancing the Diffusion of Foreign Ions on α-Al_2O_3 Grain Boundaries," J. Amer. Ceram. Soc. 81, 305-14 (1998).
50. B. A. Pint, "The Oxidation Behavior of Oxide-Dispersed β-NiAl: I. Short-Term Cyclic Data and Scale Morphology," Oxidation of Metals, 49 (1998) 531-60.
51. N. Hiramatsu and F. H. Stott, "The Effect of Lanthanum on the Scales Developed on Thin Foils of Fe-20Cr-5Al at Very High Temperatures," Oxid. Met., 51 (1999) p.479-94.
52. J. P. Wilber, M. J. Bennett and J. R. Nicholls, "Life-time Extension of Alumina Forming FeCrAl-RE alloys: Influence of Alloy Thickness," Mater. High Temp., 17 125-32 (2000).
53. P. F. Tortorelli, B. A. Pint, E. A. Kenik, K. L. More, and I. G. Wright, "Oxide Defects and Damage Processes in Iron-Based Alumina-Formers," Mater. Sci. Forum, 369-372 337-44 (2001).
54. D. Naumenko, W. J. Quadakkers, V. Guttman, P. Beaven, H. Al-Badairy, G. J. Tatlock, R. Newton, J. R. Nicholls, G. Strehl, G. Borchardt, J. Le-Coze, B. Jönsson, A. Westerlund, "Critical Role of Minor Element Constituents on the Lifetime Oxidation Behaviour of FeCrAl(RE) Alloys," in Lifetime Modelling of High Temperature Corrosion Processes, M. Schütze, W. J. Quadakkers, J. R. Nicholls eds, p.66-82, Maney, London, 2001.
55. D. Naumenko, J. Le-Coze, E. Wessel, W. Fischer, W. J. Quadakkers, "Effect of Trace Amounts of Carbon and Nitrogen on the High Temperature Oxidation Resistance of High Purity FeCrAl Alloys," Mater. Trans., 43 168-72 (2002).
56. P. Untoro, M. Dani, H. J. Klaar, J. Mayer, D. Naumenko, J. C. Kuo, W. J. Quadakkers, "The Effect of Trace Amounts of Mg in FeCrAl Alloys on the Microstructure of the Protective Alumina Surface Scales,"; pp.271-8 in *Materials Aspects in Automotive Catalytic Converters*. Edited by H. Bode. Wiley-VCH, Weinheim, Germany, 2002.
57. W. J. Quadakkers, J. Nicholls, D. Naumenko, J. Wilber and L. Singheiser, "Factors Affecting Oxide Growth Rates and Lifetime of FeCrAl Alloys,"; pp.93-105 in *Materials Aspects in Automotive Catalytic Converters*. Edited by H. Bode. Wiley-VCH, Weinheim, Germany, 2002.
58. D. P. Whittle and J. Stringer, "Improvement in Properties: Additives in Oxidation Resistance," Philos. Trans. R. Soc. London, A, 295 309-29 (1980).
59. E. Lang (Ed.), *The Role of Active Elements in the Oxidation Behavior of High Temperature Metals and Alloys* . Elsevier Applied Science, London, U.K., 1989.
60. W. E. King (Ed.), Mater. Sci. Forum, Vol. 43, *The Reactive Element Effect on High Temperature Oxidation -- After Fifty Years*. Trans Tech Publications, Winterthur, Switzerland, 1989.

61. B. A. Pint, "Experimental Observations in Support of the Dynamic Segregation Theory to Explain the Reactive Element Effect," Oxid. Met., 45 1-37 (1996).
62. B. A. Pint, “Progress in Understanding the Reactive Element Effect Since the Whittle and Stringer Literature Review,” in Proceedings of the John Stringer Symposium. Edited by P. F. Tortorelli and P. Y. Hou. ASM, Materials Park, OH, in press.
63. K. P. R. Reddy, J. L. Smialek and A. R. Cooper, "^{18}O Tracer Studies of Al_2O_3 Scale Formation on NiCrAl Alloys," Oxid. Met., 17 429-49 (1982).
64. B. A. Pint, J. R. Martin and L. W. Hobbs, "^{18}O/SIMS Characterization of the Growth Mechanism of Doped and Undoped α-Al_2O_3," Oxid. Met., 39 167-95 (1993).
65. R. Prescott, D. F. Mitchell, M. J. Graham and J. Doychak, "Oxidation Mechanisms of β-NiAl+Zr Determined by SIMS," Corr. Sci., 37 1341-64 (1995).
66. B. A. Pint, P. F. Tortorelli and I. G. Wright, "Effect of Cycle Frequency on High Temperature Oxidation Behavior of Alumina-Forming Alloys," Oxid. Met., 58 73-101 (2002).
67. I. G. Wright, B. A. Pint, L. M. Hall and P. F. Tortorelli, "Experimental Results and Modeling Related to Oxidation Lifetimes,"; pp.339-58 in *Lifetime Modelling of High Temperature Corrosion Processes*. Edited by M. Schütze, W. J. Quadakkers and J. R. Nicholls. Maney, London, 2001.
68. B. A. Pint, I. G. Wright and P. F. Tortorelli, Oak Ridge National Laboratory internal report, submitted 2002.
69. B. A. Pint, K. L. More and I. G. Wright, “The Role of Hafnium on the Growth and Adhesion of Alumina Scales,” manuscript in progress.
70. J. Doychak, NASA Lewis Research Center, Cleveland, OH, unpublished research, 1993.
71. B. A. Pint, L. R. Walker and I. G. Wright, “Characterization of the Breakaway Al Content in Alumina-Forming Alloys,” Mater. High Temp., in press (2003).
72. W. J. Quadakkers and M. J. Bennett, "Oxidation Induced Lifetime Limits of Thin Walled, Iron Based, Alumina Forming, Oxide Dispersion Strengthened Alloy Components," Mater. Sci. Tech., 10 126-31 (1994).
73. J. L. Smialek, D. T. Jayne, J. C. Schaeffer and W. H. Murphy, "Effects of Hydrogen Annealing, Sulfur Segregation and Diffusion on the Cyclic Oxidation Resistance of Superalloys: A Review," Thin Solid Films, 253 285-92 (1994).
74. C. Sarioglu, C. Stinner, J. R. Blachere, N. Birks, F. S. Pettit and G. H. Meier, "The Control of Sulfur Content in Nickel-Base Single Crystal Superalloys and Its Effects on Cyclic Oxidation Resistance,"; pp.71-80 in *Superalloys 1996*. Edited by R. D. Kissinger, D. J. Deye, D. L. Anton, A. D. Cetel, M. V. Nathal, T. M. Pollack, D. A. Woodford. TMS, Warrendale, PA, 1996.
75. J. L. Smialek, "The Effect of Hydrogen Annealing on the Impurity Content of Alumina-Forming Alloys," Oxid. Met., 55 75-86 (2001).

76. J. L. Smialek and B. A. Pint, "Optimizing Scale Adhesion for Single Crystal Superalloys," Mater. Sci. Forum, 369-372 459-66 (2001).

77. B. A. Pint, K. L. More, P. F. Tortorelli, W. D. Porter and I. G. Wright, "Optimizing the Imperfect Oxidation Performance of Iron Aluminides," Mater. Sci. Forum, 369-372 411-8 (2001).

78. B. A. Pint and I. G. Wright, "Cyclic Oxidation Behavior of cast NiCrAl Alloys,"; pp.263-74 in Electrochemical Society Proceedings, Vol.98-9. *High Temperature Corrosion and Materials Chemistry*. Edited by P. Y. Hou, M. J. McNallan, R. Oltra, E. J. Opila and D. A. Shores. Electrochemical Society, Pennington, NJ, 1998.

79. D. K. Gupta and D. S. Duvall, "A Silicon and Hafnium Modified Plasma Sprayed MCrAlY Coating for Single Crystal Superalloys," pp.711-20 in Proceedings of the 5th International Symposium on Superalloys, *Superalloys 1984*. Edited by M. Gell, et al. TMS-AIME, Warrendale, PA, 1984.

80. I. G. Wright and B. A. Pint, "Some effects of interactions among minor element additions on the high-temperature oxidation behavior of Ni-base alumina-forming alloys,"; pp.86-87 in Proc. SF2M 2000, Journées d'automne, Société Française de Métallurgie et de Matériaux, Paris, 2000.

81. H. E. Evans and M. P. Taylor, "Diffusion Cells and Chemical Failure of MCrAlY Bond Coats in Thermal-Barrier Coating Systems," Oxid. Met., 55 17-34 (2001).

82. J. L. Smialek, J. A Nesbitt, C. A. Barrett and C. E. Lowell, "Cyclic Oxidation Testing and Modelling: A NASA Lewis Perspective,"; pp.148-68 in *Cyclic Oxidation of High Temperature Materials*. Edited by M. Schütze and W. J. Quadakkers. Institute of Materials, London, U.K., 1999.

83. H. Hindam and D. P. Whittle, "Peg Formation by Short-Circuit Diffusion in Al_2O_3 Scales Containing Oxide Dispersions," J. Electrochem. Soc., 129 1147-9 (1982).

84. A. Czyrska-Filemonowicz, R. A. Versaci, D. Clemens and W. J. Quadakkers, "The Effect of Yttria Content on the Oxidation Resistance of ODS Alloys Studied by TEM,"; pp.288-97 in *Microscopy of Oxidation 2*. Edited by S. B. Newcomb and M. J. Bennett. Institute of Metals, London, U.K., 1993.

85. W. J. Quadakkers, D. Clemens and M. J. Bennett, "Measures to Improve the Oxidation Limited Service Life of Fe-Based ODS Alloys,"; pp.195-206 in *Microscopy of Oxidation 3.* Edited by S. B. Newcomb and J. A. Little. Institute of Metals, London, U.K., 1997.

86. B. A. Pint and L. W. Hobbs, "Limitations on the Use of Ion Implantation for the Study of the Reactive Element Effect in β-NiAl," J. Electrochem. Soc., 141 2443-53 (1994).

87. S. B. Newcomb, R. E. Dunin-Borkowski, C. B. Boothroyd, A. Czyrska-Filemonowicz, D. Clemens and W. J. Quadakkers, "A Grain Boundary Study of the Aluminium Oxide Formed on MA956 of Different Yttria Contents,"; pp.166-76 in *Microscopy of Oxidation 3.* Edited by S. B. Newcomb and J. A. Little. Institute of Metals, London, U.K., 1997.

88. J. D. Kuenzly and D. L. Douglass, "The Oxidation Mechanism of Ni_3Al Containing Yttrium," Oxid. Met., 8 139-178 (1974).

89. H. E. Evans, "Stress Effects in High Temperature Oxidation of Metals," Inter. Mater. Rev., 40 1-40 (1995).

90. H. E. Evans, J. R. Nicholls and S. R. J. Saunders, "The Influence of Diffusion-Related Mechanisms in Limiting Oxide-Scale Failure," Solid State Phenom., 41 137-56 (1995).

91. J. Quadakkers and L. Singheiser, "Practical Aspects of the Reactive Element Effect," Mater. Sci. Forum, 369-72 77-92 (2001).

92. B. A. Pint, K. B. Alexander, O. R. Monteiro and I. G. Brown, "An Oxygen Potential Gradient as a Possible Diffusion Driving Force,"; pp.497-502 in Materials Research Society Symposia Proceedings, Vol.527, *Diffusion Mechanisms in Crystalline Materials*. Edited by Y. Mishin, G. Vogl, N. Cowern, R. Catlow and D. Farkas. MRS, Pittsburgh, PA, 1998.

Table I. Chemical composition (in atomic%) of cast FeCrAl alloys obtained by inductively coupled plasma analysis and combustion analysis.

Dopant:	undoped	0.1Y	0.035Y	0.05Hf	0.1Hf	Mm
Fe	70.30	69.83	70.10	70.08	69.99	70.31
Cr	20.13	20.21	20.08	19.83	19.93	19.58
Al	9.56	9.86	9.77	9.98	9.97	10.03
Ni	<0.01	<0.01	0.01	<0.01	<0.01	<0.01
Si	<0.01	<0.01	<0.01	<0.01	<0.01	<0.01
Ti	<0.01	<0.01	<0.01	<0.01	<0.01	<0.01
Y	<0.01	**0.08**	**0.035**	<0.01	<0.01	<0.01
Zr	<0.01	<0.01	<0.01	<0.01	<0.01	<0.01
Hf			<0.01	**0.053**	**0.097**	0.006
Other			0.01 Mo			**0.02 Ce**
						0.007 Nd
					0.004 La	
B	<0.002	<0.05	<0.002	0.01	<0.01	0.014
P	<0.003	<0.003	0.007	<0.003	0.005	<0.003
C	<0.04	<0.04	0.0044	0.04	<0.04	0.04
N(ppma)	<10	11	11	<10	<10	11
O(ppma)	92	115	65	91	65	65
S(ppma)	85	16	<4	41	39	20

Table II. Chemical composition (in atomic%) of cast co-doped FeCrAl alloys obtained by inductively coupled plasma analysis and combustion analysis.

Dopant:	0.14 Hf+Y	0.038 Hf+Y	0.020 Hf+Y	0.018Hf+Y	0.06Zr+Y
Fe	69.58	70.08	69.58	69.75	70.21
Cr	20.32	20.07	20.28	20.15	20.06
Al	9.90	9.79	10.09	9.98	9.62
Ni	<0.01	0.01	0.01	<0.01	<0.01
Si	<0.01	<0.01	<0.01	<0.01	<0.01
Ti	<0.01	<0.01	<0.01	<0.01	<0.01
Y	**0.09**	**0.003**	**0.002**	**<0.01**	**<0.01**
Zr	<0.01	<0.01	<0.01	<0.01	**0.063**
Hf	**0.05**	**0.035**	**0.018**	**0.018**	
Other	0.01 Cu				
B	<0.002	0.005	0.005	<0.002	0.019
P	<0.003	<0.01	0.005	0.005	0.010
C	0.04	<0.04	0.0100	0.0938	0.0078
N(ppma)	11	<10	15	<10	11
O(ppma)	85	69	39	124	98
S(ppma)	15	16	16	59	34

Table III. Parabolic rate constants (g^2/cm^4s) and activation energy (kJ/mol) for several FeCrAl alloys.

Temperature:	undoped FeCrAl	0.08Y	0.038Hf+Y	0.020 Hf+Y
1000°C	3.1×10^{-13}	$1.1\text{-}2.0 \times 10^{-13}$	4.8×10^{-14}	2.5×10^{-14}
1100°C	3.2×10^{-12}	$4.2\text{-}4.4 \times 10^{-13}$	$1.4\text{-}3.7 \times 10^{-13}$	$0.98\text{-}1.5 \times 10^{-13}$
1200°C	1.4×10^{-11}	7.5×10^{-12}	5.6×10^{-12}	3.5×10^{-12}
1300°C	$2.4\text{-}3.3 \times 10^{-11}$	$3.6\text{-}4.4 \times 10^{-11}$	$2.2\text{-}2.3 \times 10^{-11}$	1.1×10^{-11}
Activation Energy (kJ/mol)	244	352	367	366

List of Figures

Figure 1. Summary of parabolic growth rates reported in the literature.[4,6,8,13,15,18,25,27,31,32,39-41,50,53,56,68,69] The highlighted rates (diamonds) represent the lowest reported rates at 1100° and 1200°C.[8,50,69]

Figure 2. Typically relationship between reactive element addition and mass gain during 100h exposure at 1100°C (data from Ref. 8 and 69). The minimum points are for small additions of Hf which correspond to the diamonds in Figure 1.

Figure 3. Results of a screening test for different oxide dispersions in FeCrAl presented as the normalized alloy life in 1h cycles at 1200°C as a function of dopant ion size. The lifetimes were normalized to a 1.5mm specimen thickness.

Figure 4. Average parabolic rate constants for various commercial and laboratory FeCrAl compositions at 1200°C.

Figure 5. Light microscopy of the polished cross-section of the scale formed after 200h at 1200°C on FeCrAl with additions of (a) 0.05%Hf and (b) 0.08%Y.

Figure 6. Normalized lifetime for various commercial and laboratory FeCrAl compositions. Three compositions are still being tested (arrows at current status).

Figure 7. Specimen mass change during 1h cycles at 1100°C for various NiCrAl alloys.

Figure 8. Light microscopy of the polished cross-section of the scale formed after 200h at 1200°C on FeCrAl with additions of (a) 0.14%Hf/Y (b) 0.038 Hf/Y and (c) 0.020%Hf/Y.

Figure 9. Light microscopy of the polished cross-section of the scale formed after 10, 100h cycles at 1200°C on FeCrAl with additions of (a) 0.08%Y (b) 0.14%Hf/Y (c) 0.038 Hf/Y and (d) 0.020%Hf/Y.

Figure 10. Isothermal mass gains for FeCrAl alloys with and without RE additions at 1200°C plotted versus the square root of time to show the parabolic relationship.

Figure 11. Specimen mass change during 1h cycles at 1200°C for various FeCrAl alloys.

Figure 12. Total mass gain (symbols) and specimen mass change (dashed lines) during 100h cycles at 1200°C for various FeCrAl alloys. FeCrAlY shows little scale spallation during this test.

Figure 13. Total mass gain (symbols) and specimen mass change (dashed lines) during 100h cycles at 1100°C for various FeCrAl alloys.

Figure 14. Specimen mass change during 1h cycles at 1100°C for various RE-doped alloys with a base composition of Ni-7Cr-13Al.

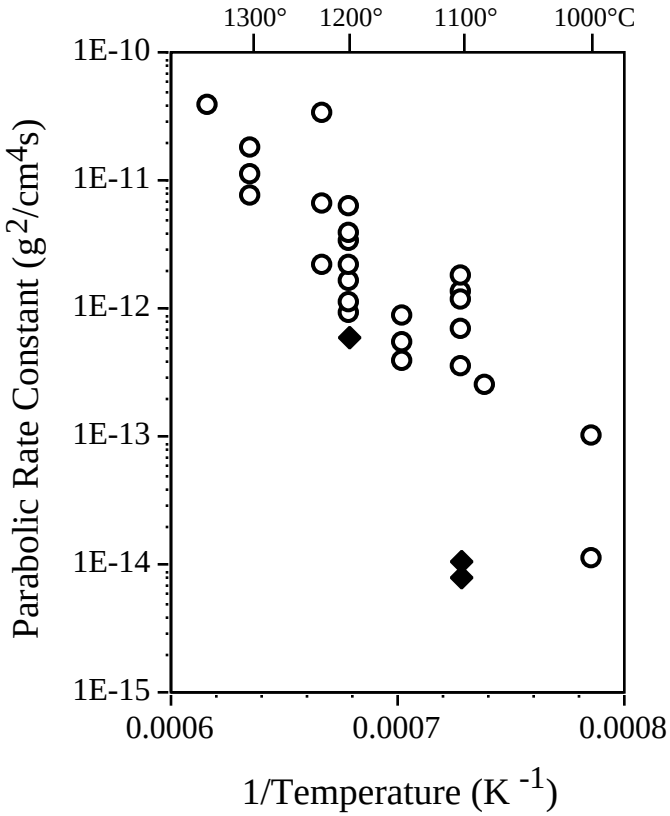

Figure 1. Summary of parabolic growth rates reported in the literature.[4,6,8,13,15,18,25,27,31,32,39-41,50,53,56,68,69] The highlighted rates (diamonds) represent the lowest reported rates at 1100° and 1200°C.[8,50,69]

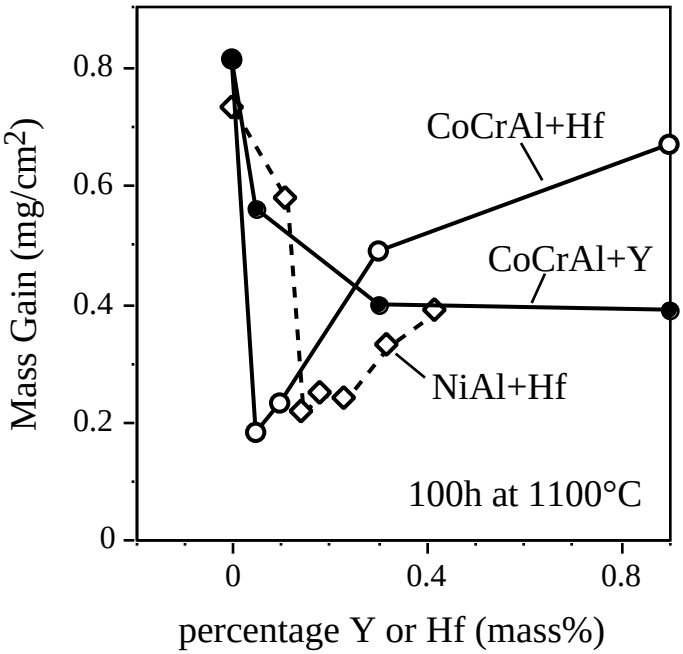

Figure 2. Typically relationship between reactive element addition and mass gain during 100h exposure at 1100°C (data from Ref. 8 and 69). The minimum points are for small additions of Hf which correspond to the diamonds in Figure 1,

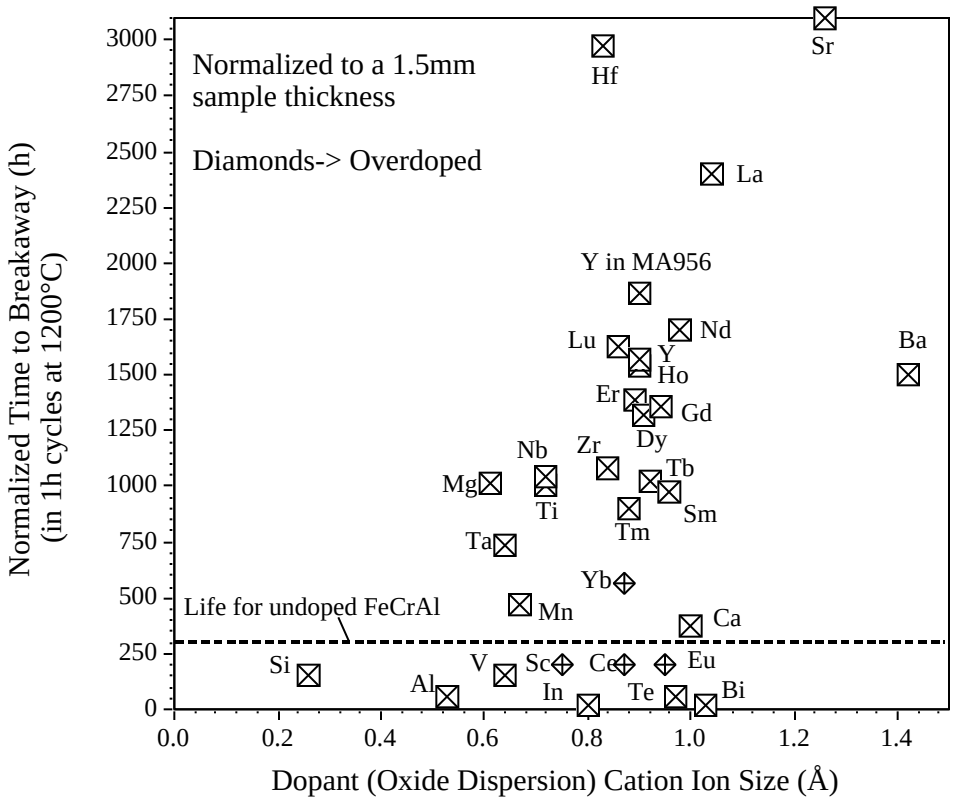

Figure 3. Results of a screening test for different oxide dispersions in FeCrAl presented as the normalized alloy life in 1h cycles at 1200°C as a function of dopant ion size. The lifetimes were normalized to a 1.5mm specimen thickness.

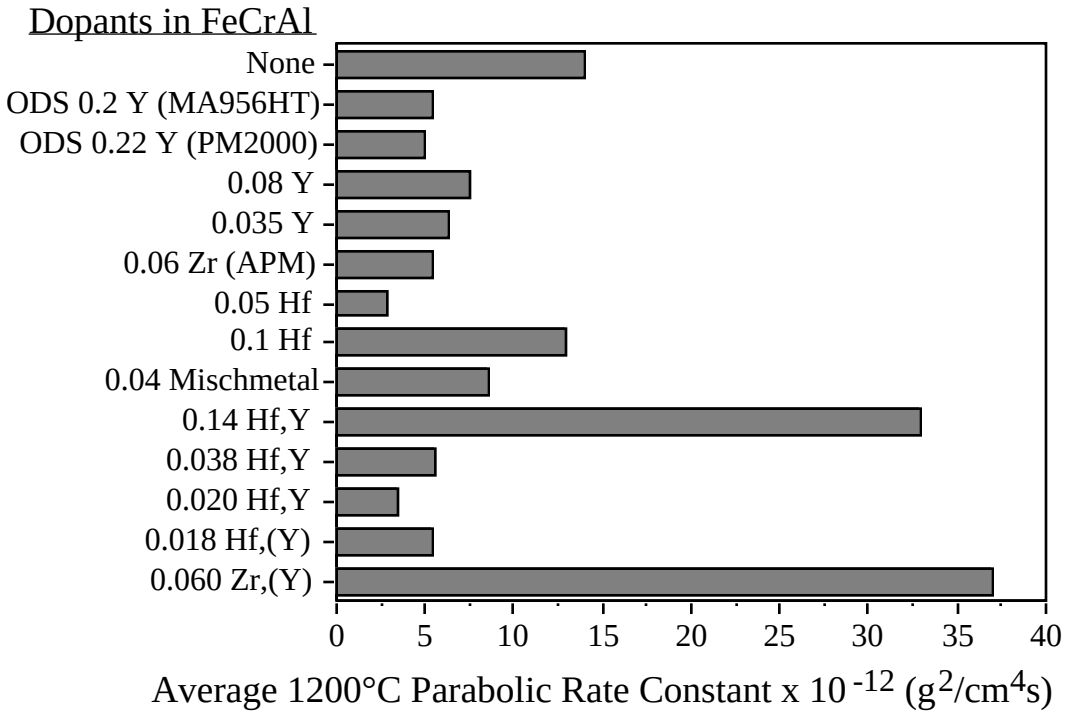

Figure 4. Average parabolic rate constants for various commercial and laboratory FeCrAl compositions at 1200°C.

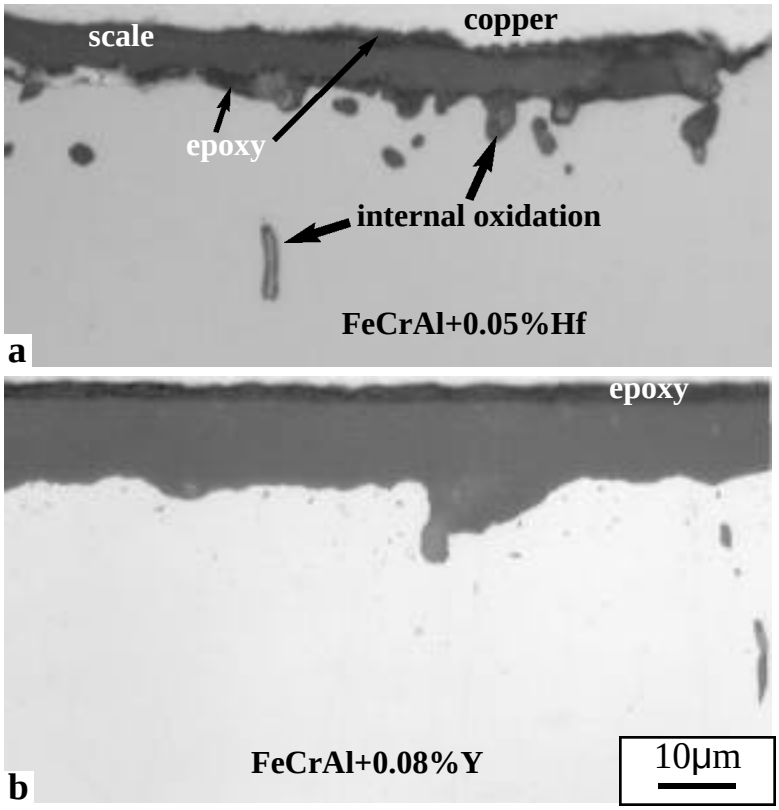

Figure 5. Light microscopy of the polished cross-section of the scale formed after 200h at 1200°C on FeCrAl with additions of (a) 0.05%Hf and (b) 0.08%Y.

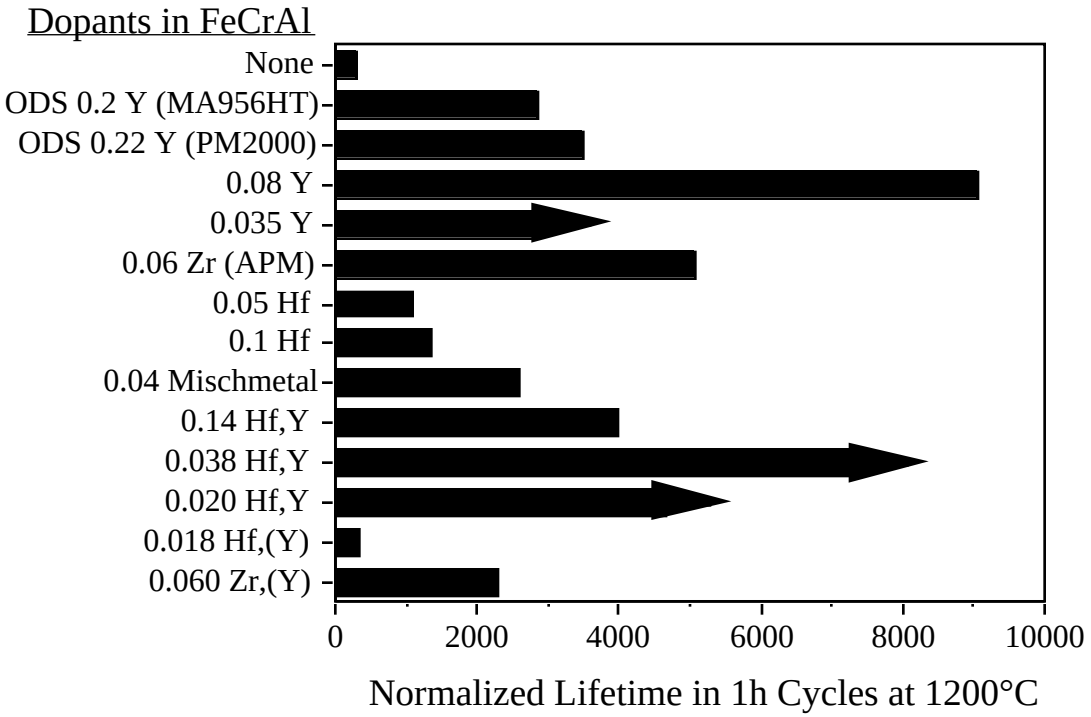

Figure 6. Normalized lifetime for various commercial and laboratory FeCrAl compositions. Three compositions are still being tested (arrows at current status).

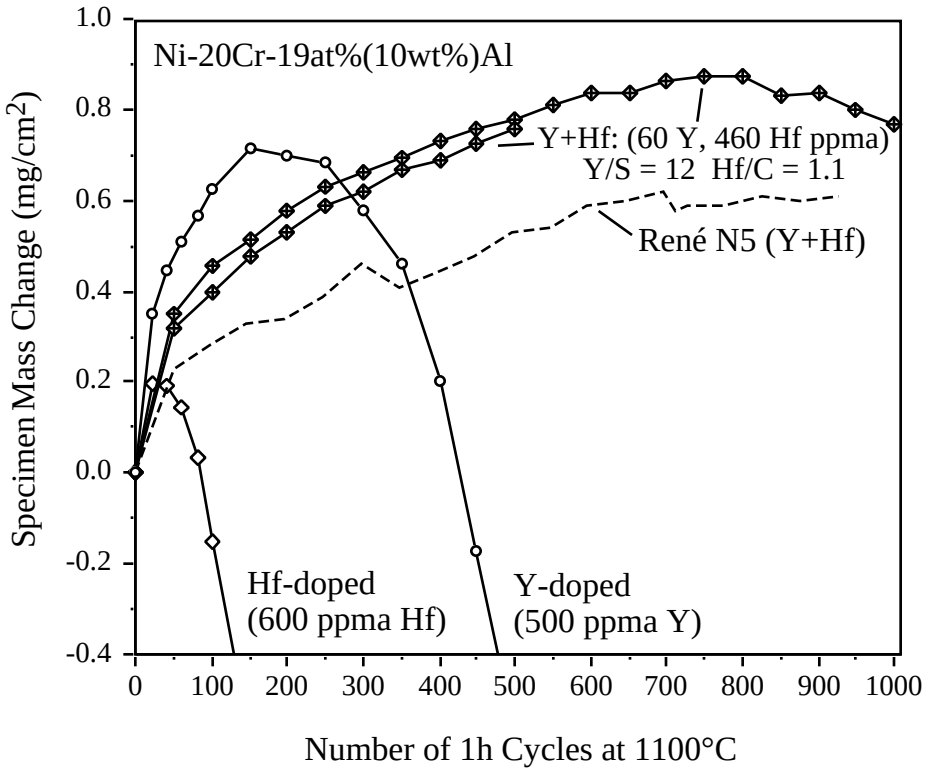

Figure 7. Specimen mass change during 1h cycles at 1100°C for various NiCrAl alloys.

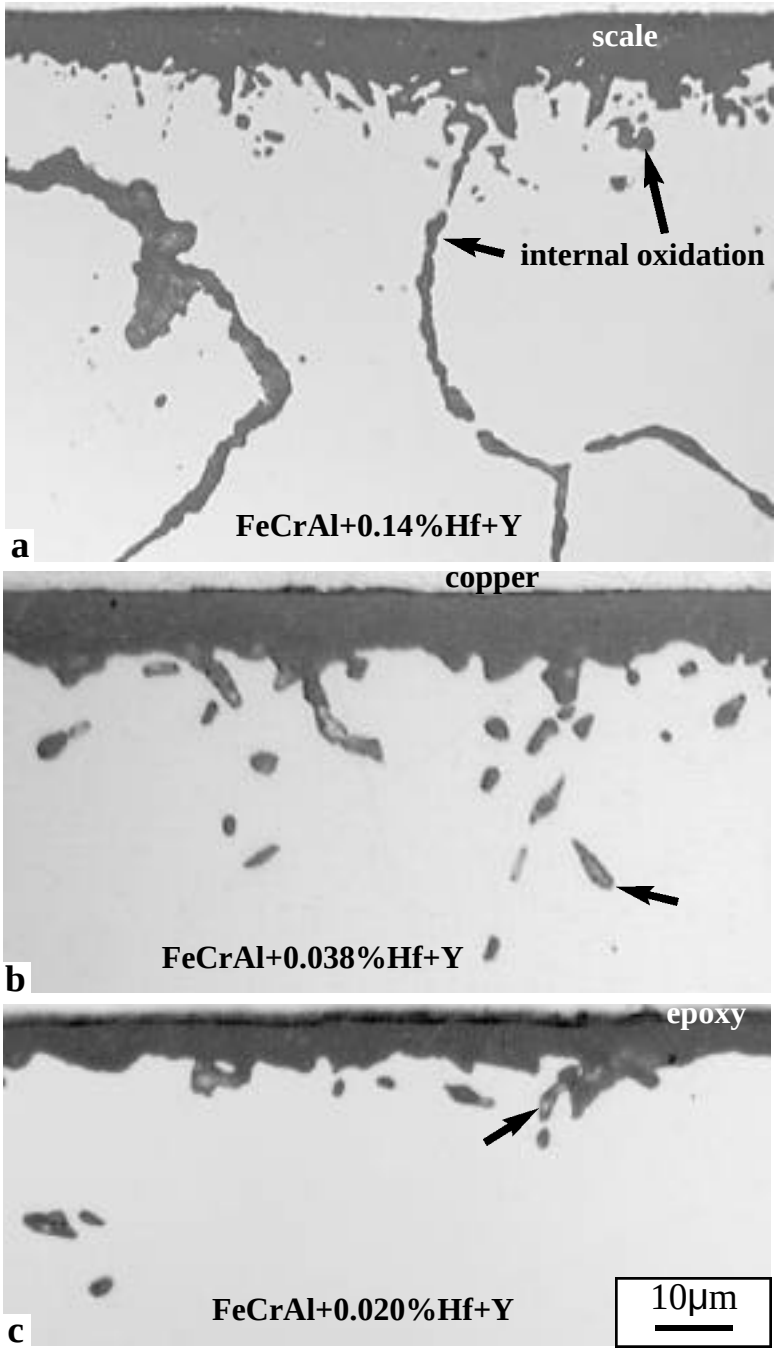

Figure 8. Light microscopy of the polished cross-section of the scale formed after 200h at 1200°C on FeCrAl with additions of (a) 0.14%Hf/Y (b) 0.038 Hf/Y and (c) 0.020%Hf/Y.

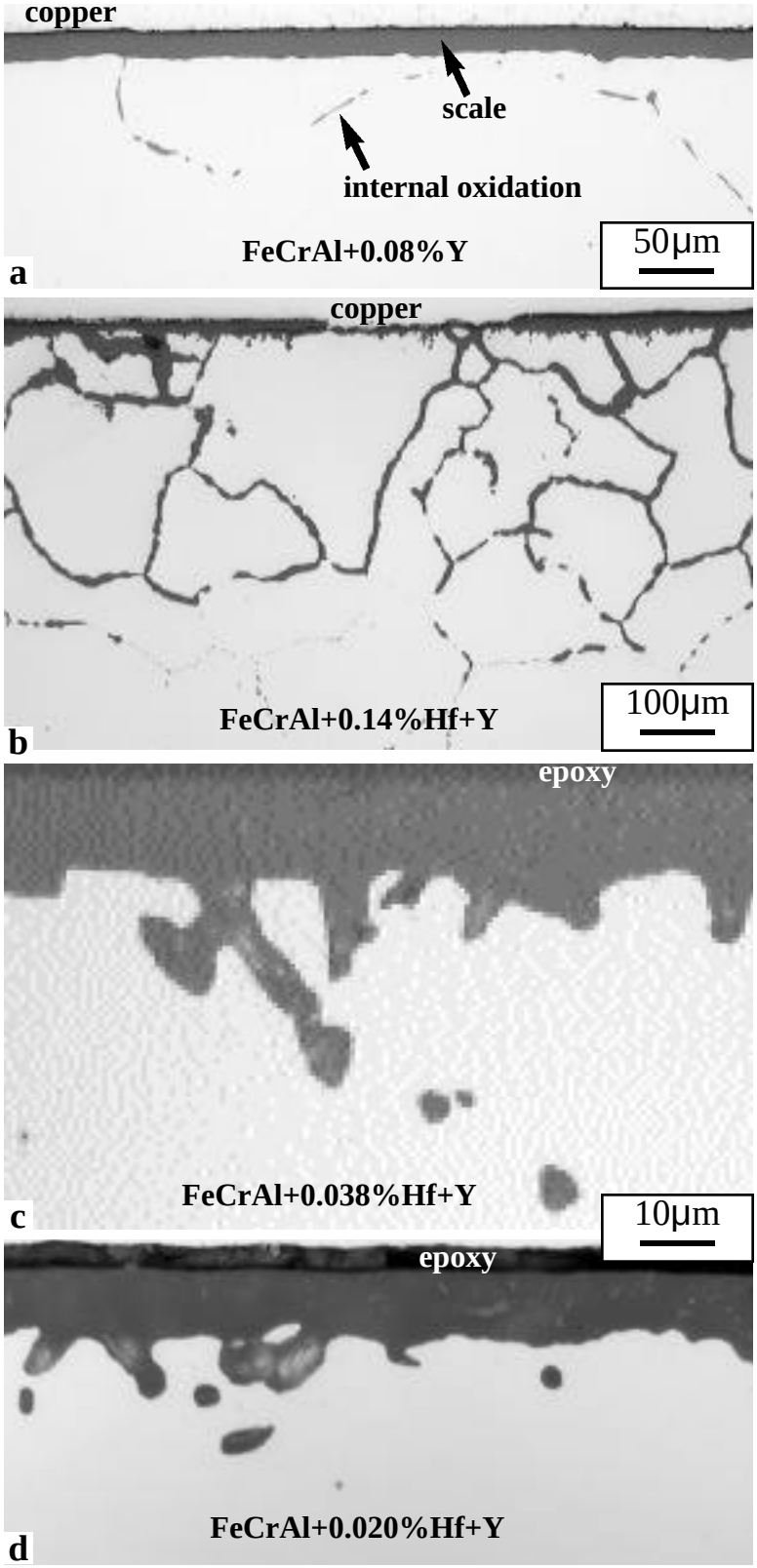

Figure 9. Light microscopy of the polished cross-section of the scale formed after 10, 100h cycles at 1200°C on FeCrAl with additions of (a) 0.08%Y (b) 0.14%Hf/Y (c) 0.038 Hf/Y and (d) 0.020%Hf/Y.

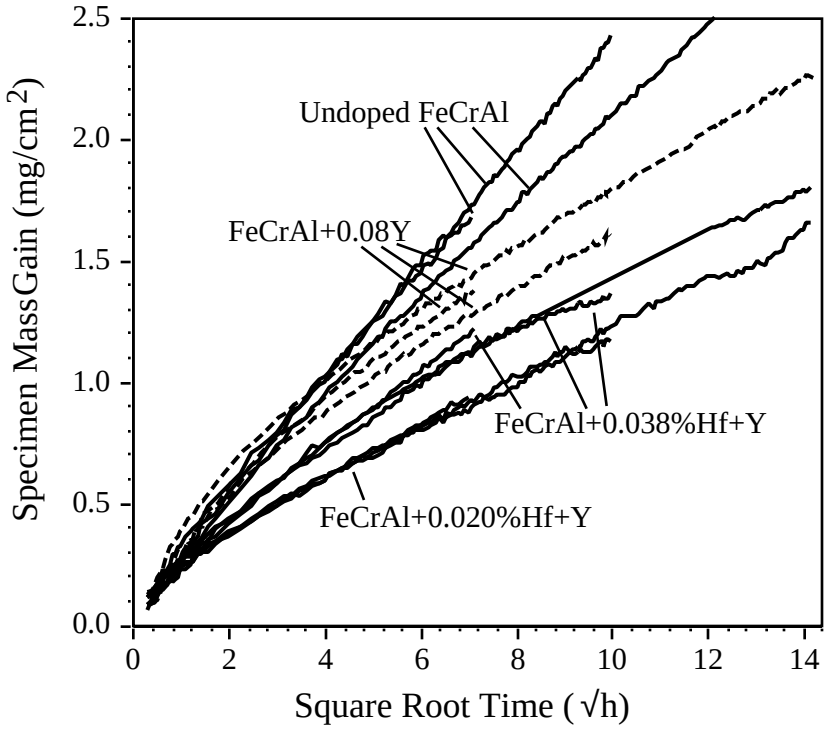

Figure 10. Isothermal mass gains for FeCrAl alloys with and without RE additions at 1200°C plotted versus the square root of time to show the parabolic relationship.

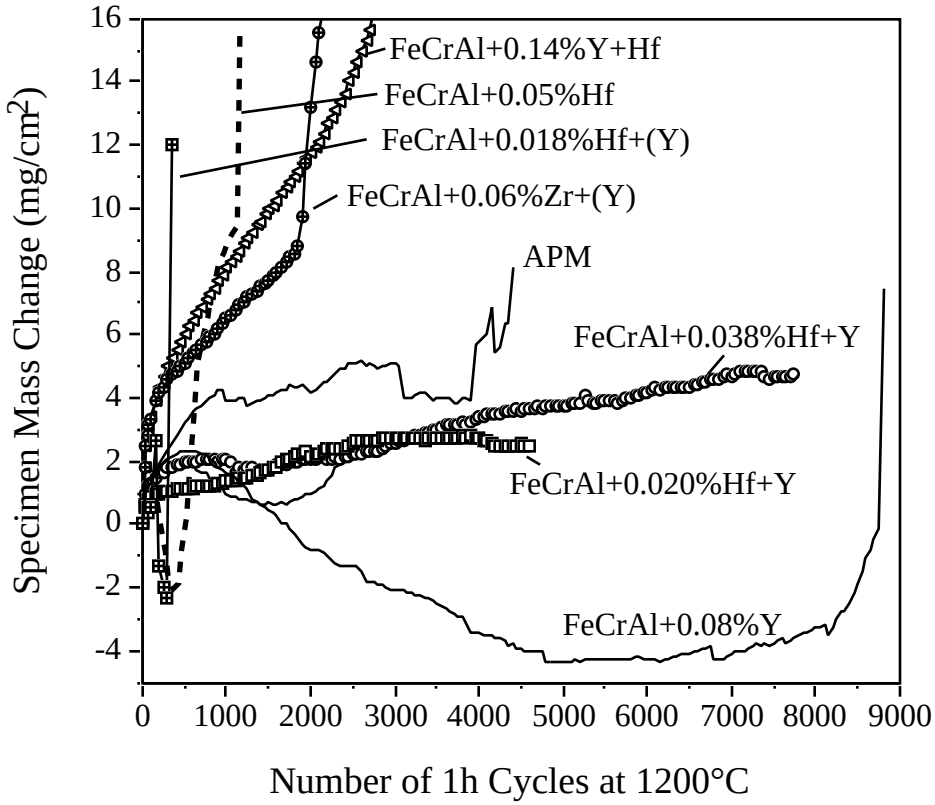

Figure 11. Specimen mass change during 1h cycles at 1200°C for various FeCrAl alloys.

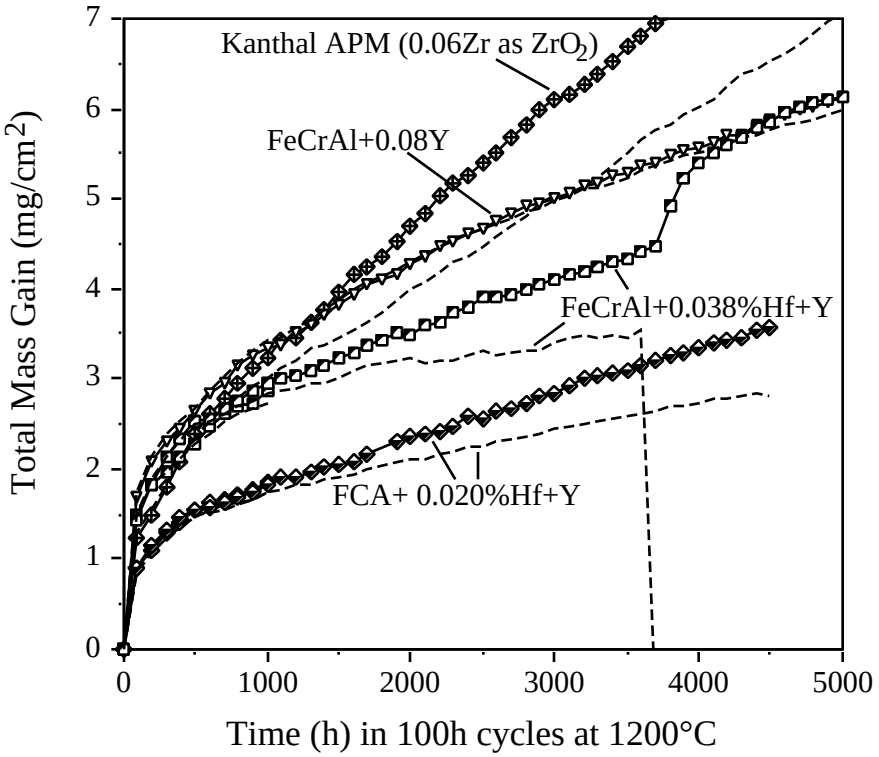

Figure 12. Total mass gain (symbols) and specimen mass change (dashed lines) during 100h cycles at 1200°C for various FeCrAl alloys. FeCrAlY shows little scale spallation during this test.

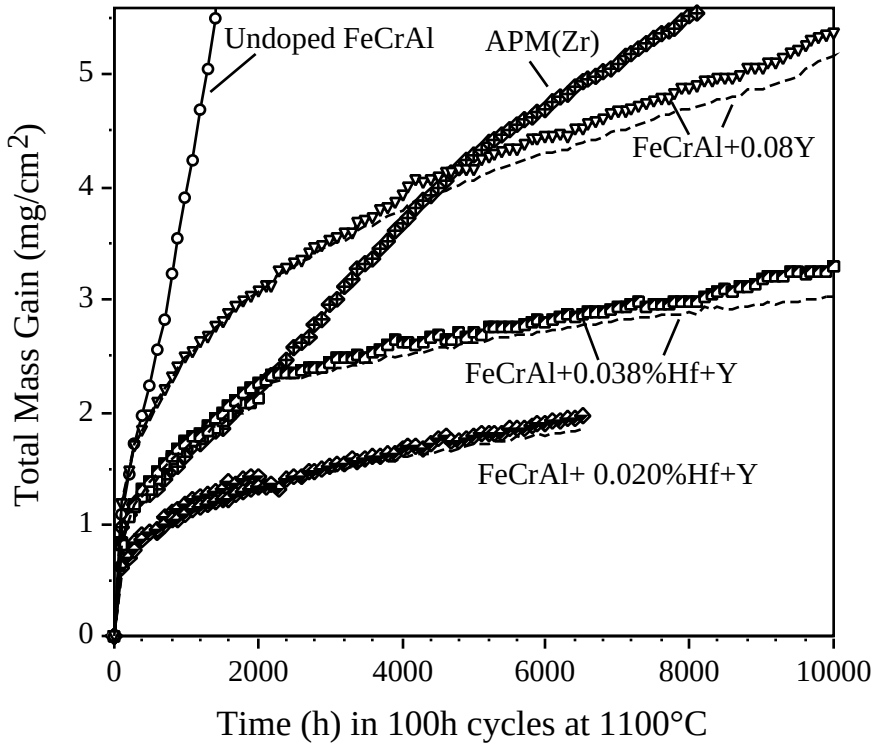

Figure 13. Total mass gain (symbols) and specimen mass change (dashed lines) during 100h cycles at 1100°C for various FeCrAl alloys.

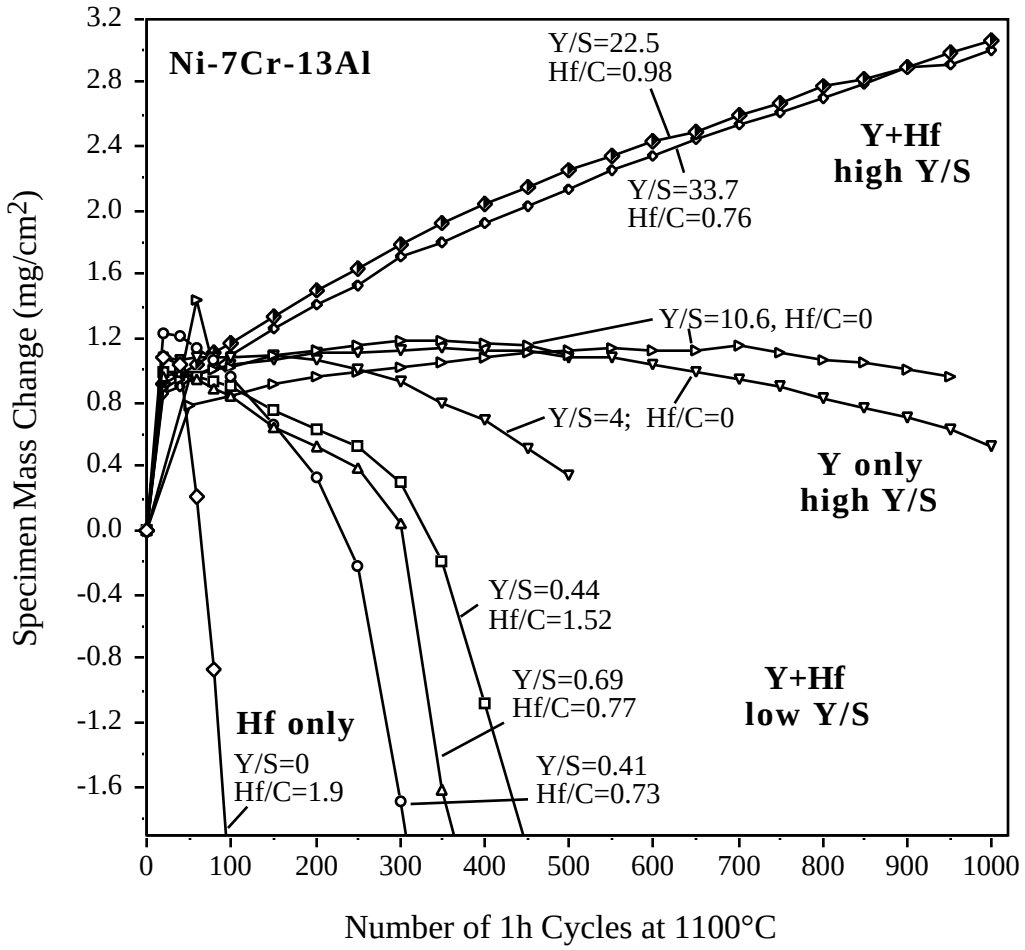

Figure 14. Specimen mass change during 1h cycles at 1100°C for various RE-doped alloys with a base composition of Ni-7Cr-13Al.